https://doi.org/10.2352/ISSN.2470-1173.2019.16.3DMP-002

4D scanning system for measurement of human body in motion

Robert Sitnik, Marta Nowak, Paweł Liberadzki and Jakub Michoński; Institute of Micromechanics and Photonics, Faculty of Mechatronics, Warsaw
University of Technology; A. Boboli 8, 02-525 Warsaw, Poland

Abstract

In this paper we propose 4DBODY system which realizes full body 4D scanning of human in motion. It consists eight measurement heads based on single frame structured light method. All heads works synchronously with frequency 120 Hz with spectral separation to eliminate crosstalk. Single frame method is based on projection of sinusoidal fringe pattern with special marker allowing for absolute phase reconstruction. We develop custom made unwrapping procedure adjusted for human body analysis. We could achieve 0.5 mm spatial resolution and 0.3 mm of accuracy within a 1.5 x 1.5 x 2.0 m^3 working volume. We integrated treadmill into system which allows to perform walking experiments. We present some results of measurements with initial validation of 4DBODY system.

Introduction

The 3D shape measurement field has significantly grown in popularity over the past few decades. The reason for this trend is the high accuracy and the high capture speed of the data [1]. Common applications include:

- biomedicine – support system for diagnosis [2,3],
- entertainment – improving the quality of animated 3D models [4,5],
- cultural heritage – digitalizing, storing and analyzing cultural heritage objects [6,7],
- law enforcement – documenting and analyzing crime scenes and reconstructing the course of accidents [8,9].

The main 3D imaging technologies used for measurements are Laser Triangulation (LT) [10,11], Time of Flight (ToF) [12,13], Structured Light (SL) [14,15] and Structure from Motion (SfM) [16,17]. LT systems are based on analysis of the deformation of lines projected from laser source onto the object. ToF sensors use light impulses and measure the return time to determine XYZ coordinates. In SL technique the deformation of a certain raster or a sequence of them on the objects surface is translated into model points. SfM is based on analyzing a sequence of images of the measured object taken from many different angles at the same time. Although these technologies are widely used in 3D imaging, they have already been introduced into commercial 4D (3D + time) measurements by companies such as 3dMD LLC [18,19], Microsoft Corporation [20,21] and Diers International GmbH [22,23]. However, there is still some space for improvement, i.e. increasing acquisition frequency or lowering the overall cost.

In this paper we present the 4DBODY scanning system. Proposed solution employs SL technique, because it provides high resolution 3D reconstruction together with high accuracy of measurements. Moreover, this approach is flexible in regard to the number of used devices that allows reasonable cost control. The 4DBODY system provide full body measurement with an accuracy up to 0.3 mm and spatial resolution up to 0.5 mm. All measurement are captured with an acquisition frequency of up to 120 Hz.

The structure of this paper is organized as follow. Following section presents system architecture and describe system components. Next section introduces developed measurement method and explain implemented algorithms. Afterwards, there is a section that discusses the initial validation of the system and shows sample movement results. The last section summarizes the study and refer to our future work.

System architecture

Presented system consists of eight measurement heads. Each measurement head consists of an industrial-class camera and a projector. Measurement heads are assembled into directional subsystems with a projector shared between two cameras. These subsystems are evenly distributed around the center of the system, as illustrated in Figure 1. In the center of the 4DBODY system we also placed the treadmill. With such setup we get the effective measurement volume of 1.5 x 1.5 x 2.0 m^3 which is sufficient for measuring most of the people.

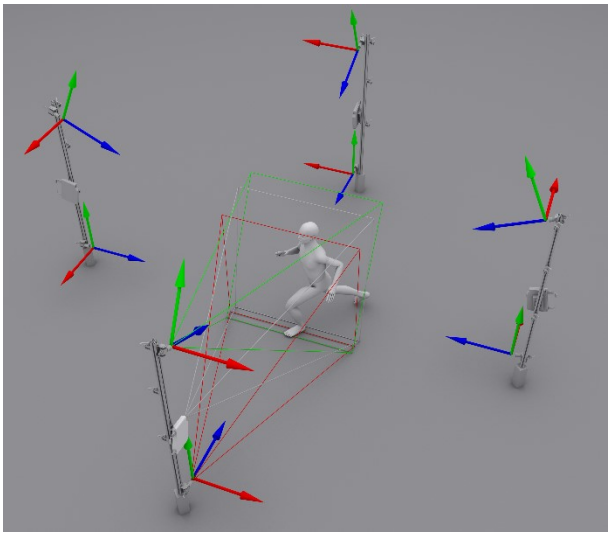

Figure 1. Architecture of 4DBODY scanning system

The projectors used in directional subsystems are Casio XJ-A242 [24] with mixed LED (red channel) and laser (blue and green channels) light sources. The detectors are FLIR Grashopper 3.0 cameras [25] providing up to 120 Hz acquisition frequency in an external trigger mode. Each projector is connected directly to its own FPGA (Field-Programmable Gate Array) integrated circuit that is responsible for both sine pattern generation and projection control. All FPGAs are connected to the Atmel AVR microcontroller broadcasting orders and spreading synchronization signal. FPGAs together with the microcontroller are the subsystem

called SM (Synchronization Module). SM provides control over both projection and acquisition but does not prevent crosstalk between directional subsystems. For this reason, the spectral separation has been employed in the presented system. This approach is realized using single channel projection (red or blue, different for neighboring projectors) and spectral filters mounted on camera lenses. The effect is displayed in Figure 2.

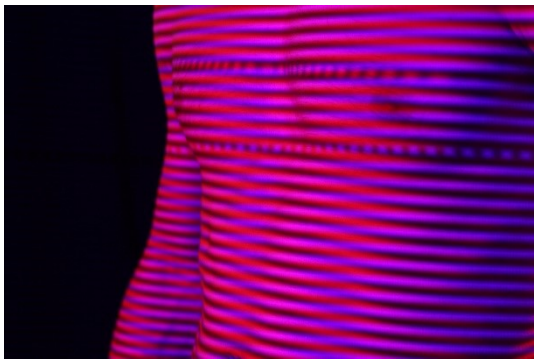

Figure 2. The effect of spectral separation displayed on measured subject

All detectors are connected to two PC-class computers that act as data servers. The dedicated application run on these computers is responsible for gathering, saving and sending captured data. Both computers are connected to TCP/IP network that enables the master unit (e.g. PC-class computer with client application) to ask for data and control the whole process. The overall control model looks as illustrated in Figure 3.

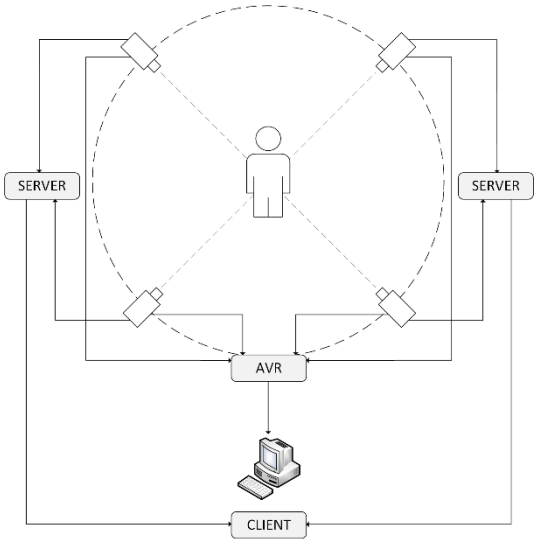

Figure 3. The overall control model in 4DBODY scanning system

With the setup described in this section we are able to capture full human body measurements at a frequency of 120 Hz. Next section provides the description for developed method and explains the path from captured image to the output point cloud.

Algorithms

The 4DBODY system employs SL single frame method. The pattern is in the form of sine fringes. This approach is similar to the method proposed by Sitnik [26]. Such patterns require an additional information to provide proper reconstruction. This information is carried in the distinguished sine fringe that is further called the marker. The modified representation of the marker is the alteration applied in our method, compared to the method proposed by Sitnik [26]. Comparison of both patterns is depicted in Figure 4.

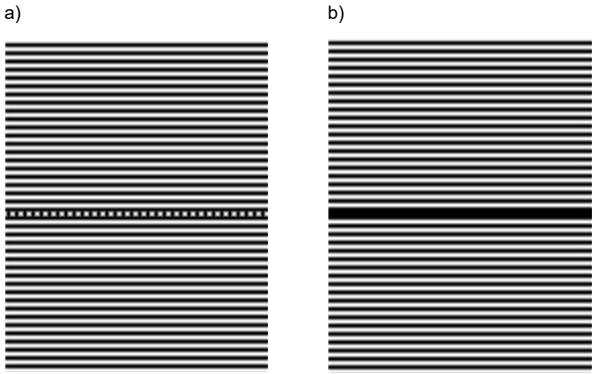

Figure 4. Comparison between sine patterns: a) the pattern that we propose; b) the pattern propose by Sitnik [26]

Captured images are further processed according to the diagram that is illustrated in Figure 5. The process begins with background separation when all pixels of analyzed surface are selected. For these pixels, the local sine fringe period is approximated. Next, modulo-2π phase is calculated simultaneously with determining pixels quality. In the following step, phase distribution is unwrapped using an information about pixel quality. Finally, the unwrapped phase is updated based on the marker localization.

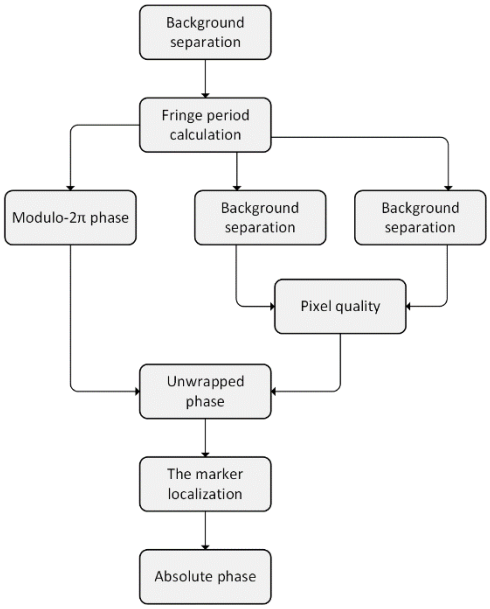

Figure 5. Diagram presenting processing steps in the 4DBODY system

The reason for background separation is limiting further calculations only to necessary pixels. Such approach significantly reduces the computing time. In this step we utilize an Otsu [27] thresholding method that is followed by morphological closing, as it is presented in Figure 6b.

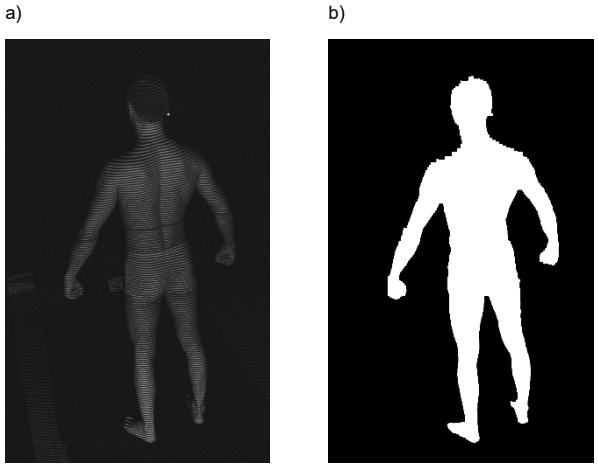

Figure 6. Effect of background separation: a) input image; b) image after background separation

Computing sine fringe period in each pixel begins with calculating local intensity median. Next, "intersections" between the median and pixel intensities in the local neighborhood are used to determine period value, as it is depicted in Figure 7a.

Modulo-2π phase is calculated using 7-point SCPS (Spatial Carrier Phase Shifting) method that was proposed by Larkin [28]. For each pixel, seven intensity values are interpolated from neighboring pixels within single sine fringe period utilizing an information received in the previous step. The effect is illustrated in Figure 7b.

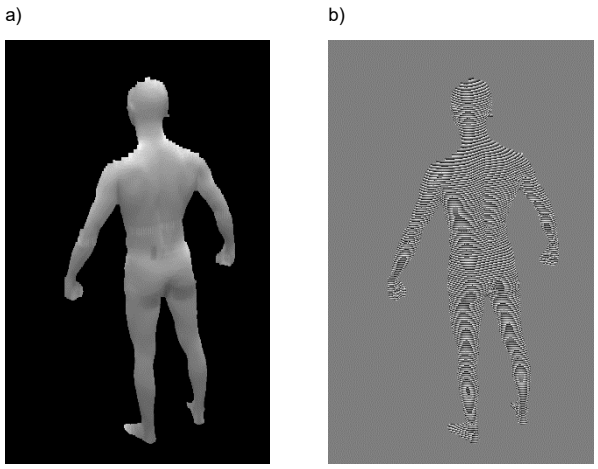

Figure 7. Effects of calculating: a) local period values; b) modulo-2π distribution

Pixel quality is determined using an information about local modulation and reliability. The modulation value in each pixel is equal to the difference between minimum and maximum intensity in the local neighborhood. Pixel reliability value is the opposite of the sum of intensity gradients from eight directions. Both modulation and reliability are normalized. Pixel quality is calculated as an average of its modulation and reliability, as it is presented in Figure 8a. Such approach allows us to assign low quality to areas:

- with a low contrast of sine fringes – due to low modulation value,
- that are close to separated background border – due to low modulation value,
- with local discontinuities – due to low reliability value,
- with local fringe distortions – due to high reliability values.

Phase unwrapping begins with spanning "edges" between neighboring (only in vertical and horizontal direction) pixels. An edge is spanned from and to certain pixel index. Its quality is calculated according to Equation (1).

$$Q_{e(p_1,p_2)} = \frac{Q_{p_1} + Q_{p_2}}{2} - \sqrt{|Q_{p_1} - Q_{p_2}|} \quad (1)$$

where:

$e(p_1, p_2)$ – an edge between pixel p_1 and pixel p_2,
Q_p – quality of a pixel p,
$Q_{e(p_1,p_2)}$ – quality od an edge.

The $\sqrt{|Q_{p_1} - Q_{p_2}|}$ part is responsible for reduction of the importance of edges with high difference between "from" and "to" pixels. The edges are then sorted by quality. The unwrapping process begins with an edge of the highest quality. Both pixels are unwrapped and added to the same segment. For each next edge:

- if none of its pixels belong to any segment then they are unwrapped in reference to each other and create a new segment,
- if one of its pixels belong to any segment then the other pixel value is unwrapped and this pixel is added to first pixels segment,
- if both of its pixels belong to any segment then they are unwrapped in reference to a pixel of larger segment and the smaller segment is added to the larger segment.

Unwrapping is finished when there are no more edges to analyze. The effect of this process is illustrated in Figure 8b.

Figure 8. Effects of calculating: a) pixel quality; b) unwrapped phase distribution

The marker localization begins with performing one-dimensional FFT (Fast Fourier Transform) [29,30]. Sine fringes are filtered out in the spectral domain. After an adequate inverse FFT, followed by thresholding and segmentation, the left-over pixels belong to the marker, as it is depicted in Figure 9a. Marker pixels are used to calculate the marker phase value that result in determining the marker fringe number. The difference between determined and real marker fringe number allows calculating the necessary phase shift.

The absolute phase distribution is calculated by applying this phase shift to the unwrapped phase distribution. The effect of this operation is presented in Figure 9b.

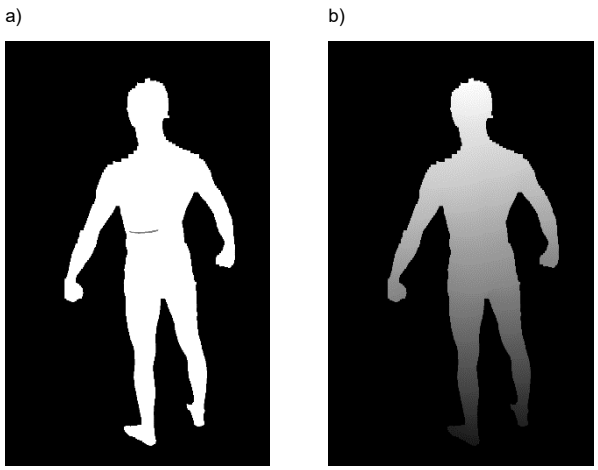

Figure 9. Effect of calculating: a) the marker position; b) absolute phase distribution

The output point cloud is calculated from the absolute phase distribution. Image pixels are scaled into real-world XYZ coordinates based on directional subsystem calibration data. Clouds from individual subsystems are merged into one multidirectional cloud.

Initial validation and results

Recommendations for SL systems validation are specified in VDI/VDE 2617-6 [31]. In 4DBODY system, because of the dynamic character of the measurement, we decided to simplify this process in order to perform an initial validation. We used a model of a known geometry that we attached to a turntable. The model is in the form of a 1.1 x 1.8 m^2 glass board, covered in a white, matt paper. Measurements of rotating model were taken in the moment when the model was oriented diagonally in the measurement volume. One measurement was also taken when the model was frontal to the measuring subsystem. We calculate the RMS value of fitting a virtual plane to received point clouds as a measure of error. The resulting, average (for all directional subsystems) RMS error is 0.21 mm.

We also examined 4DBODY system on several people doing different, basic movements. The resulting, multidirectional point clouds consist of about 4 million points. The average point-to-point distance is about 0.5 mm. For each point, we calculate XYZ coordinates, lightness and normal vector. Several frames of exemplary measurements are presented in Figure 10 and Figure 11.

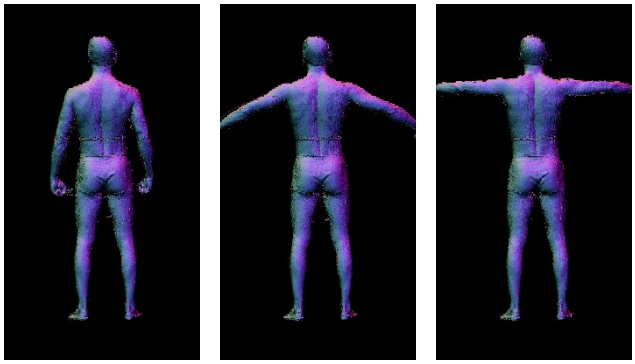

Figure 10. Three frames from a measurement of a subject raising his shoulders

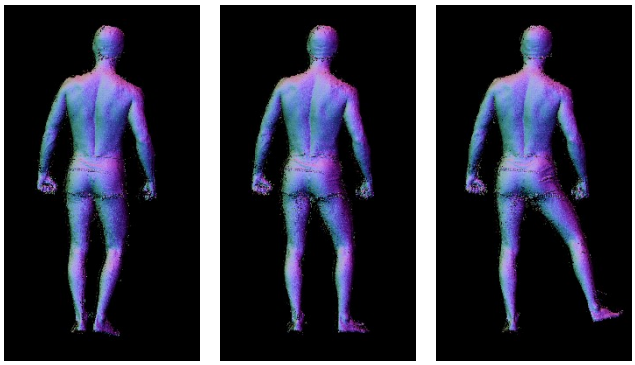

Figure 11. Three frames from a measurement of a subject raising his leg

Conclusions

We developed the 4DBODY system that provide full, human body measurement with a frequency of up to 120 Hz. The output point cloud contains about 4 million points per frame, with an accuracy below 0.3 mm. Furthermore, point cloud is easily scaled into other data types such as triangle mesh what makes it possible to use in many applications. Marker-less measurement, together with these features create a potential for the 4DBODY system to be used in numerous medical applications, e.g. supporting rehabilitation process. Moreover, the output data can also be used in computer graphics in the process of creating reliable and ready-to-use animated 3D models.

In the future works, we plan to further increase system accuracy and acquisition frequency. We also want to optimize our algorithms to achieve near real-time reconstruction.

Acknowledgements

The work described in this article was part of the project PBS3/B9/43/2015, funded by the National Centre for Research and Development with public money for science and statutory work at Warsaw University of Technology.

References

[1] S. Zhang, "High-speed 3D shape measurement with structured light methods: A review," Optics and Laser Engineering, vol. 106, July 2018, pp. 119-131, 2018.

[2] P. Treleaven, J. Wells, "3D body scanning and healthcare applications," Computer, vol. 40, no. 7, pp. 28-34, 2007

[3] S. Paśko, M. Dzierzęcka, H. Purzyc, A. Charuta, K. Barszcz, B. Bartyzel, M. Komosa, „The Osteometry of Equine Third Phalanx by the Use of Three-Dimensional Scanning: New Measurement Possibilities", Scanning, vol. 2017, pp. 1-6, 2017

[4] V. Kasapakis, E. Dzardanova, D. Gavalas, S. Sylaiou, "Remote synchronous interaction in mixed reality gaming worlds," in Proceedings of the 10th International Workshop on Immersive Mixed and Virtual Environment Systems, Amsterdam, Netherlands, 2018.

[5] G. Kontogianni, A. Georgopoulos, "Developing and exploiting textured 3D models for a serious game application," in Proceedings of the 8th International Conference on Virtual Worlds and Games for Serious Applications, Barcelona, Spain, 2016.

[6] C. W. Khong, M. A. M. Pauzi, "The user experience of 3D scanning tangible cultural heritage artifacts," in Proceeding of International Conference on Human Systems Engineering and Design: Future Trends and Applications", Reims, France, 2018.

[7] C. Little, D. Patterson, B. Moyle, A. Bec, "Every footprint tells a story: 3D scanning of heritage artifacts as an interactive experience," in Proceedings of the Australasian Computer Science Week Microconference, Brisband, Queensland, Australia, 2018.

[8] T. J. U. Thompson, P. Norris, "A new method for the recovery and evidential comparison of footwear impressions using 3D structured light scanning," Science & Justice, vol. 58, no. 3, pp. 237-243, 2018.

[9] D. Raneri, "Enhancing forensic investigation through the use of modern three-dimensional (3D) imaging technologies for crime scene reconstruction," Australian Journal of Forensic Science, vol. 50, no. 6, pp. 697-707, 2018.

[10] M. A. B. Ebrahim, "3D laser scanners' technologies overview," International Journal of Science and Research, vol. 4, no. 10, pp. 323-331, 2015.

[11] M. Hess, A. Baik, "3D laser scanning," Digital techniques for documenting and preserving cultural heritage, pp. 199-206, 2017.

[12] Y. Cui, S. Schuon, D. Chan, S. Thrun, C. Theobalt, "3D shape scanning with a time-of-flight camera," in Proceedings of IEEE Computer Society Conference on Computer Vision and Pattern Recognition, San Francisco, USA, 2010.

[13] C. Schaller, J. Penne, J. Hornegger, "Time-of-flight sensor for respiratory motion gating," Medical Physics, vol. 35, no. 7, pp. 3090-3, 2008.

[14] W. Yin, S. Feng, T. Tao, M. Trusiak, Q. Chen, C. Zuo, "High-speed 3D shape measurement using the optimized composite fringe patterns and stereo-assisted structured light system," Optics Express, vol. 27, no. 3, pp. 2411-2431, 2019.

[15] J. Geng, "Structured-light 3D surface imaging: a tutorial," Advances in Optics and Photonics, vol. 3, no. 2, pp. 128-160, 2011.

[16] M. Hernandez, T. Hassnerm J. Choi, G. Medioni, "Accurate 3D face reconstruction via prior constrained structure from motion," Computer & Graphics, vol. 66, pp. 14-22, 2017.

[17] S. Zuffi, A. Kanazawa, M. J. Black, „Lions and tigers and bears: capturing non-rigid, 3D, articulated shape from images," in Proceedings of IEEE Conference on Computer Vision and Pattern Recognition, Salt Lake City, Utah, USA, 2018.

[18] C. Zhang, S. Pujades, M. Black, G. Pons-Moll, "Detailed, accurate human shape estimation from clothed 3D scan sequences," in Procedings of IEEE Conference on Computer Vision and Pattern Recognition, Honolulu, USA, 2017.

[19] C. Lane, W. E. Harrell, "Completing the 3-dimensional picture," American Journal of Orthodontics and Dentofacial Orthopedics, vol. 133, no. 4, pp. 612-620, 2008.

[20] A. Collet, M. Chuang, P. Sweeney, D. Gillett, D. Evseev, D. Calabrese, H. Hoppe, A. Kirk, S. Sullivan, "High-quality streamable free-viewport video," ACM Transactions on Graphics, vol. 34, no. 4, 2015.

[21] H. Nguyen, Z. Wang, P. Jones, B. Zhao, "3D shape, deformation and vibration measurements using infrared Kinect sensors and digital image correlation," Applied Optics, vol. 56, no. 32, pp. 9030-9037, 2017.

[22] C. Draus, D. Moravec, A. Kopiec, P. Knott, "Comparison of barefoot vs. shod gait on spinal dynamics using DIERS Formetric 4D and DIERS Pedoscan systems," Open Journal of Therapy and Rehabilitation, vol. 3, no. 3, pp. 70-76, 2015.

[23] B. Degenhardt, Z. Starks, S. Bhatia, G. A. Franklin, "Appraisal of the DIERS method for calculating postural measurements: an observational study," Scoliosis and Spinal Disorders 12:28, 2017.

[24] Informational material, Casio, https://www.casio.com/products/projectors/slim-projectors/xj-a242 (accessed on 26 February 2019)

[25] Informational material, FLIR, https://www.ptgrey.com/grasshopper3-23-mp-mono-usb3-vision-sony-pregius-imx174-camera (accessed on 26 February 2019)

[26] R. Sitnik, "Four-dimensional measurement by a single-frame structured light method," Applied Optics, vol. 48, pp. 3344-3354, 2009.

[27] N. Otsu, "A threshold selection method from gray-level histograms," IEEE Transactions on systems, man and cybernetics, vol. 9, pp. 62-66, 1979.

[28] M. Takeda, "Spatial-carrier fringe-pattern analysis and its applications to precision interferometry and profilometry: an overview," Industrial Metrology, vol. 1, no. 2, pp. 79-99, 1990.

[29] G. D. Bergland, "A guided tour of the fast Fourier Transform," IEEE Spectrum, vol. 6, no. 7, pp. 41-52, 1969.

[30] R. C. Singleton, "On computing the fast Fourier Transform," CACM, vol. 10, pp. 153-161, February 1971.

[31] VDI/VDE 2617-6: Accuracy of CMMs—Guideline for the application of ISO 10360 to CMMs with optical distance sensors, https://www.vdi.de/uploads/tx_vdirili/pdf/9778569.pdf (accessed on 26 February 2019).

Author Biography

Robert Sitnik (Member of OSA and SPIE) received his MSc Eng (1999), PhD (2002) in applied optics from the Warsaw University of Technology. He has authored and co-authored more than hundred scientific papers. His interests are structured light shape measurement (3D/4D), triangulation methods, digital image processing, computer graphics, animation software development and virtual reality techniques. He has been a leader of projects from various fields like 3D optical metrology, virtual and augmented reality and supporting medical diagnosis by opto-numerical solutions. He is head of Virtual Reality Techniques Division at WUT.

Marta Nowak is a PhD student at Warsaw University of Technology, Warsaw, Poland. She obtained her M.Sc. Eng. degree in Mechatronics, specialization Multimedia Techniques, from Warsaw University of Technology in 2015. Her research interests include point cloud processing and analysis, 3D modeling, parametric surfaces, computer animation, and machine vision.

Paweł Liberadzki received his MSc Eng (2014) in automatic control from the the Warsaw University of Technology. He is currently doing his PhD in Virtual Reality Techniques Division of Warsaw University of Technology. His interests are structured light technologies (3D/4D), computer graphics and software engineering. He has taken part in several projects employing 3D imaging techniques to human body measurements.

Jakub Michoński received his MSc Eng (2011) in applied optics from the Warsaw University of Technology. His interests include analysis of static and dynamic point cloud measurements of the human body, computer graphics, computer vision in quality inspection and software and systems engineering. He has extensive experience in development of robust, complete data analysis and visualization software used in numerous fields: medicine, cultural heritage, forensic science and quality inspection. Long-standing associate of the Optographx research group at the Institute of Micromechanics and Photonics.

JOIN US AT THE NEXT EI!

IS&T International Symposium on

Electronic Imaging

SCIENCE AND TECHNOLOGY

Imaging across applications . . . Where industry and academia meet!

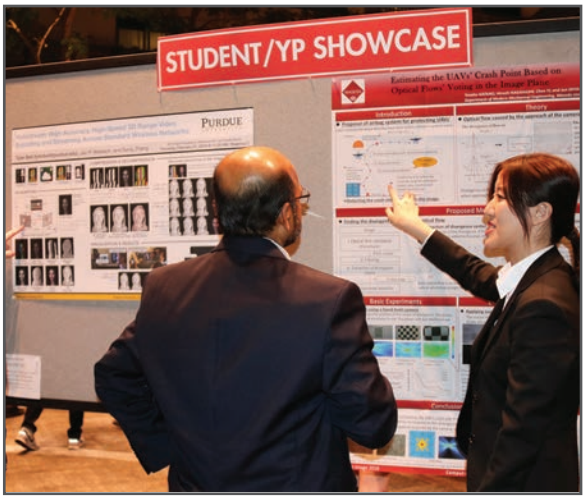

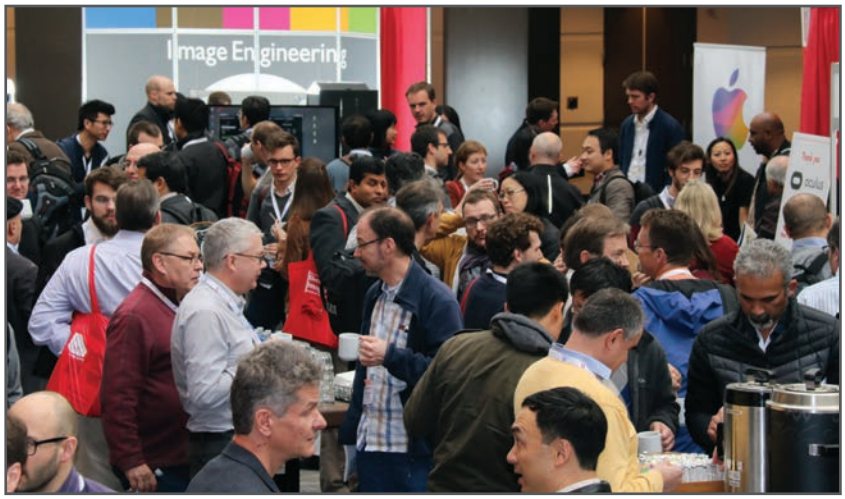

• SHORT COURSES • EXHIBITS • DEMONSTRATION SESSION • PLENARY TALKS •
• INTERACTIVE PAPER SESSION • SPECIAL EVENTS • TECHNICAL SESSIONS •

www.electronicimaging.org

IS&T
imaging.org